^{77}Se-NMR evidence for spin-singlet superconductivity with exotic superconducting fluctuations in FeSe

J. Li,[1] B. L. Kang,[1] D. Zhao,[1] B. Lei,[2] Y. B. Zhou,[1] D. W. Song,[1] S. J. Li,[1] L. X. Zheng,[1] L. P. Nie,[1] T. Wu,[1,2,3,4,*] and X. H. Chen[1,2,3,4,5,†]

[1]*Hefei National Laboratory for Physical Sciences at the Microscale, University of Science and Technology of China, Hefei, Anhui 230026, China*

[2]*CAS Key Laboratory of Strongly-Coupled Quantum Matter Physics, Department of Physics, University of Science and Technology of China, Hefei, Anhui 230026, China*

[3]*CAS Center for Excellence in Superconducting Electronics (CENSE), Shanghai 200050, China*

[4]*Collaborative Innovation Center of Advanced Microstructures, Nanjing University, Nanjing 210093, China*

[5]*CAS Center for Excellence in Quantum Information and Quantum Physics, Hefei, Anhui 230026, China*

(Received 27 September 2021; revised 4 February 2022; accepted 7 February 2022; published 23 February 2022)

Although the nature of the superconducting state has been intensively studied in FeSe, many fundamental issues including the pairing symmetry and superconducting fluctuations are still highly controversial. Here, we report a revised ^{77}Se-nuclear magnetic resonance (NMR) study on the superconducting state of ^{77}Se-enriched bulk FeSe. Below the superconducting temperature (T_c), by carefully avoiding the rf heating effect, a remarkable linewidth broadening and obvious reduction of the Knight shift are observed under external magnetic field along both in-plane and out-of-plane directions, suggesting an intrinsic superconducting nature. These exotic results unambiguously rule out the possibility of chiral *p*-wave pairing, and favor a pairing scenario with the mixing of $s^{\pm}$ and *d* wave. A slight decrease of the Knight shift well above T_c is also revealed under a moderated external magnetic field, suggesting exotic superconducting fluctuations beyond phase fluctuations in the two-dimensional limit. These renewed NMR results provide valuable constraints for the theoretical models on the exotic superconductivity in FeSe.

DOI: 10.1103/PhysRevB.105.054514

I. INTRODUCTION

Due to strongly electronic correlations and multiband/orbital character, iron-based superconductors (IBSCs) offer an excellent chance to explore the exotic nature of unconventional superconductivity [1–6]. In particular, in bulk FeSe as the simplest IBSC, since a small Fermi energy (E_F) accompanied with a relatively large superconducting gap Δ leads to a considerable $\frac{\Delta}{E_F}$ with the value of $\sim$0.1 [7,8], the superconducting pairing mechanism may be at the crossover from Bardeen-Cooper-Schrieffer to Bose-Einstein condensation (BCS-BEC), which is featured by the preempted superconducting fluctuations and pseudogaplike behavior [9–14]. Moreover, orbital-selective electronic correlations and superconducting pairings are also revealed in bulk FeSe [15–18], and the cooperation of electronic nematicity and spin-orbit interaction could lead to nematic superconductivity [19–22]. Taking into account all these facts, several unconventional superconducting pairing mechanisms have already been proposed, including the mixing of *s*-wave and *d*-wave pairing, the nematic pairing with orbital-selective spin fluctuations, time-reversal-symmetry-breaking (TRSB) nematic superconductivity, and so on [23–25]. Clarifying the exact pairing symmetry would be the first step to pin down the pairing mechanism and understand the exotic nature of superconductivity in bulk FeSe [26].

Although the nature of the superconducting state in bulk FeSe has been intensively studied, many controversies on the pairing symmetry and superconducting fluctuations remain [5,6]. For example, the exact form of the superconducting gap structure (e.g., the existence of the gap nodes) is still elusive [27–30]; the thermodynamic evidence for the preempted superconducting fluctuations, the high field induced Fulde-Ferrell-Larkin-Ovchinnikov state, and the *B* phase are still lacking [10–13,31]. In addition, some experimental results indicate the possible realization of *p*-wave or TRSB Cooper pairing in bulk FeSe [19,32,33]. However, the debate on sample quality (i.e., the amounts of defects and domain boundaries) makes no conclusion on this issue [5,6,33]. All in all, more insightful information is needed to shed light on the above debates.

II. EXPERIMENTAL DETAILS

By utilizing the coupling between the electronic spins and the nuclear spins, nuclear magnetic resonance (NMR) provides key information on both local and thermodynamic properties for superconductivity. Previously, only the remarkable reduction of the nuclear spin-lattice relaxation rate ($\frac{1}{T_1T}$) below T_c is a well-established NMR manifestation for the

*wutao@ustc.edu.cn
†chenxh@ustc.edu.cn

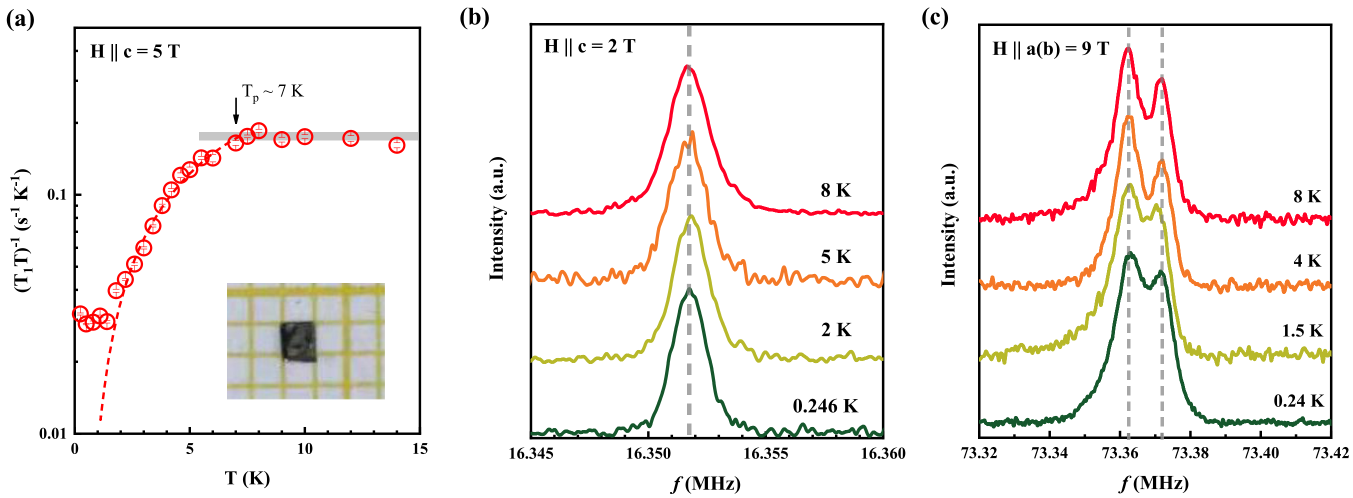

FIG. 1. Nuclear spin-lattice relaxation and NMR spectra measurements on the superconducting transition of bulk FeSe by utilizing optimized rf pulses. (a) Temperature-dependent $\frac{1}{T_1T}$. T_p is the onset of the decrease of $\frac{1}{T_1T}$. The inset shows the photograph of the measured sample. (b),(c) NMR spectra deep inside the superconducting state of the bulk FeSe. The nearly unchanged spectra are incomprehensible as the missing of the expected Redfield pattern (see Supplemental Material for a detailed analysis).

superconducting transition in bulk FeSe [Fig. 1(a)]. However, except for the loss of spectral intensity, the usual manifestation of the superconducting state in NMR spectra is almost absent in previous ^{77}Se-NMR investigations including linewidth broadening and reduction of spin susceptibility [Figs. 1(b) and 1(c)] [34–36]. In light of the rf-pulse heating effects in the superconducting state of Sr_2RuO_4 [37,38], it is necessary to reexamine the NMR experiment in the superconducting state of the bulk FeSe by carefully excluding the rf-pulse heating effects. In fact, as shown in Figs. 1(b) and 1(c), the temperature-independent NMR linewidth across T_c is very unusual by considering the magnetic field distribution in the vortex-lattice state (see Supplemental Material for details [39]; also see Refs. [40–45] therein). Here, by adopting a sufficiently low-power rf pulse, we have revisited the NMR spectra in the superconducting state of bulk FeSe down to the lowest temperature (~0.24 K) in a ^{3}He cryostat. Considering the significant loss of NMR spectral intensity in the superconducting state, our main NMR studies are conducted on a ^{77}Se-enriched (50%) FeSe single crystal. In our experiments, clear reductions of Knight shift and remarkably skewed broadening of the NMR spectra are observed in the superconducting state under both in-plane and out-of-plane magnetic fields. In the following sections of this paper, we will present detailed experimental data and analysis. Experimental settings and methods can be found in the Supplemental Material [39].

III. RESULTS AND DISCUSSION

With applying an in-plane magnetic field along the orthorhombic crystallographic $a(b)$ axis [$H \parallel a(b)$], the rf-pulse heating effect is characterized and presented in Fig. 2(a). The rf-pulse energy is characterized by the energy of the π pulse and is denoted as E_π, where the $\frac{\pi}{2}$ pulse energy is $\frac{E_\pi}{2}$ (for details, see Supplemental Material [39]). Following a typical rf-pulse heating effect in the spin-singlet pairing superconducting state [46,47], the NMR spectra measured with smaller E_π move to the lower frequency. When E_π is sufficiently small (<58 μJ), the NMR spectra remain unchanged with further decreasing E_π, which suggests that the superconducting state is no longer affected by the rf-pulse heating effect [37,38]. As shown in Fig. 2(a), the NMR spectra with a strong rf pulse ($E_\pi > 540$ μJ) exhibit a clear double-peak structure, which resembles the splitting due to the formation of nematic domains in the normal state. With lowering the energy of the rf pulse, such a double-peak structure is smeared out by the linewidth broadening effect in the vortex-lattice state. Fitting with the sum of Lorentzian peak functions, we find that the intensity ratio of the low- to high-frequency peak (I_l/I_h) decreases drastically with decreasing E_π. This suggests a greater suppression of I_l in the superconducting state due to the nematic nature of the superconductivity [48]. Figure 2(b) presents the intrinsic temperature-dependent NMR spectra across the superconducting transition; a greater suppression of I_l is also observed with lowering the temperature [48]. We obtain a reduction of the Knight shift: $\Delta K|_{H\parallel a(b)} = K_h(8\text{ K}) - K_h(0.24\text{ K}) \sim 0.009\%$ from the fitted peaks in Fig. 2(b), where K_h is the Knight shift of the high-frequency peak. As marked by the dashed lines in Fig. 2(b), the nearly unchanged splitting of the low- and high-frequency peaks indicates that nematicity induced anisotropy seems not to be affected by the developing of superconductivity. These results are consistent with a recent NMR investigation reported by Vinograd *et al.* [49] (presented in the Supplemental Material [39]). Next, we present our main results of the NMR study with applying $H||c$.

First, as shown in Fig. 3(a), the rf-pulse heating effect manifests itself as distinct E_π-dependent NMR lines. The NMR line measured under a strong rf pulse is symmetric and apparently narrower, while for the NMR line that represents the intrinsic superconducting state, one observes significant asymmetric broadening and an obvious left shift of the peak position. This character has also been confirmed in a high-quality nonenriched sample [39]. As shown in Fig. 3(b), the temperature-dependent NMR spectra measured with avoiding rf-pulse heating also reflects a typical behavior of the NMR

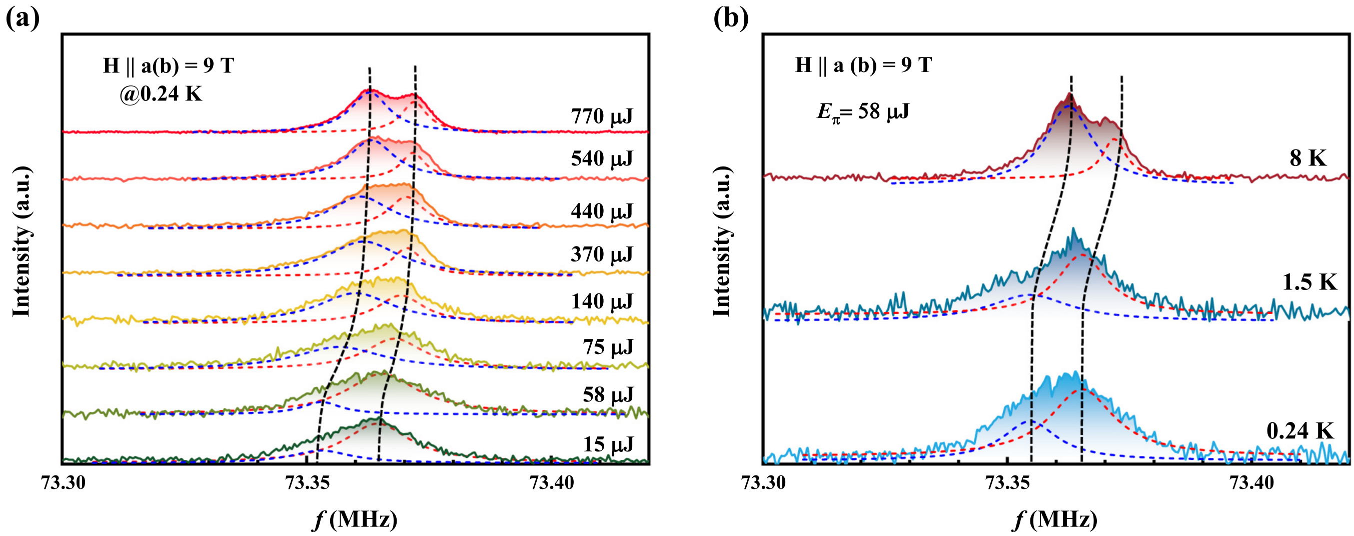

FIG. 2. Characterization of the rf-pulse heating effects and the evolution of the intrinsic NMR spectra in the superconducting state with $H\|(b)$. (a) rf-pulse energy-dependent NMR spectra. The two fitted Lorentzian peaks are shown as the blue and red dashed lines. The black dashed lines track the peak positions which represent the NMR spectra of the two orthogonal nematic domains. (b) Temperature-dependent NMR spectra measured with fixed unheated rf-pulse energy.

spectra across a singlet-pairing superconducting transition [46,47].

Within the measuring condition of Fig. 3(a), FeSe is in the vortex-lattice state [31], and the significant broadening of the NMR spectra straightforwardly suggests a prominent inhomogeneity. The same feature has also been observed with H parallel to Fe-Se-Fe direction as reported by Vinograd *et al.* [49]. The apparently skewed distribution with a long high-frequency tail is reminiscent of the Redfield pattern, which is produced by the specific local field distribution $h_l(r)$ of the vortices [50]. Previous scanning tunneling microscopy (STM) measurements observed a hexagonal vortex-lattice structure in bulk FeSe [51]. Figure 3(d) demonstrates the simulated $h_l(r)$, in which we also adopt a hexagonal vortex-lattice structure

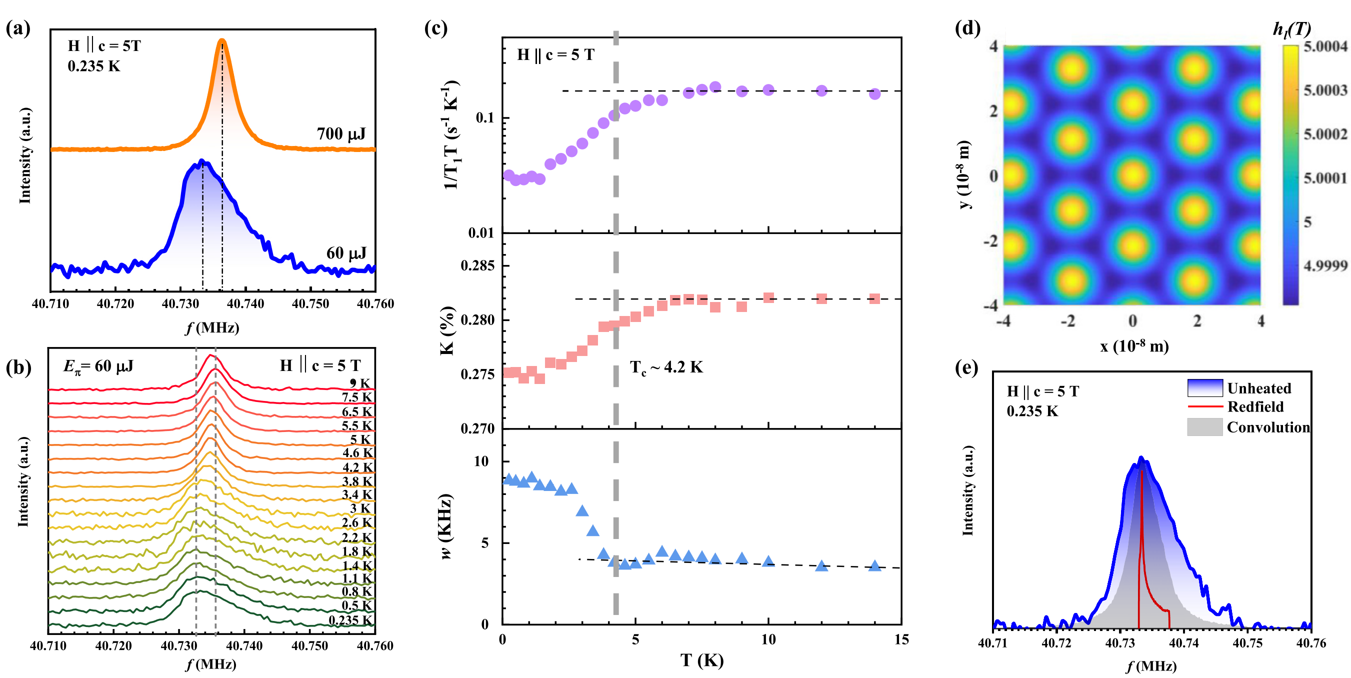

FIG. 3. Intrinsic NMR characterization on the superconducting transition with $H \parallel c$. (a) Comparison of the NMR spectra measured with heated and unheated rf pulse. The dash-dotted lines indicate the peak positions of the heated and unheated spectra. (b) Temperature-dependent NMR spectra measured with unheated rf-pulse condition. The vertical dashed lines draw the peak-frequency range of the temperature-dependent NMR spectra. (c) Comparison among $\frac{1}{T_1T}(T)$, $K(T)$, and $w(T)$. Dashed lines are a guide for the eye. (d) 2D color map of the simulated $h_l(r)$. (e) Comparison among the observed NMR line (blue), the simulated Redfield pattern (red), and the calculated convolution (shaded area).

(for details, see Supplemental Material [39]). As shown in Fig. 3(e), comparing with the measured NMR spectra, broadenings contributed by the simulated Redfield pattern are rather small, e.g., $\gamma^{77}(h_{l\max} - h_{l\min})|_{H\|c,\,5T} \sim 4.2$ KHz. Convoluting with the normal-state NMR line, $h_l(r)$ could only slightly change the normal-state NMR line which still deviates from the skewed broadening of the superconducting-state NMR line (see details in the Supplemental Material [39]). Note that, due to the nematic superconductivity, the vortices in FeSe have an elongated structure: the coherence length along the longer axis (ξ_L) is larger than the shorter one (ξ_s) by a factor of ∼2 [51]. In this case, $h_l(r)$ should be described by the anisotropic Ginzburg-Landau equations [52]. Previously, only a symmetric broadening NMR line shape has been observed in the underdoped iron-pnictide family with the superconducting states coexisting with nematic order [53,54]. Whether or not such a nematic superconductivity in FeSe could take responsibility for the remarkably skewed broadening is still elusive. In addition, for bulk FeSe, the above skewed distribution in NMR spectra is also immune to defects since it exhibits almost the same structure in low- and high-T_c samples [Fig. 3(a) and Fig. S5(d)]. Furthermore, due to the absence of magnetic ordering, the large skewed distribution was ascribed to some exotic quasiparticle bound state in a recent NMR work [49].

In Fig. 3(c) we plot the temperature-dependent linewidth $w(T)$ and Knight shift $K(T)$ together with the temperature-dependent $\frac{1}{T_1T}$. Recognizing the significant upturn of $w(T)$ as the result of entering the vortex-lattice state, the onset temperature can be determined (denoted as T_c). As shown in the middle panel of Fig. 3(c), $K(T)$ begins to decrease slightly above T_c, and below T_c, the decreasing begins to accelerate. In general, $K(T)$ can be divided into two parts: $K(T) = K_s(T) + K_{\rm orb}$, where $K_s(T)$ is the temperature-dependent spin shift and $K_{\rm orb}$ is the temperature-independent orbital shift. For the spin-singlet superconducting pairing, due to the decline of the spin susceptibility, a reduction of $K_s(T)$ is expected. Meanwhile, in the mixed state of type-II superconductors, a field- and temperature-dependent diamagnetic contribution $K_{\rm dia}(H,\ T)$ should be considered [55]. Simulating with the London model with Gaussian cuts off model as presented in the Supplemental Material [39], we find that $|K_{\rm dia}| \sim 25$ ppm at the lowest temperature with $H = 5$ T ($H||c$). It only contributes about one-third of the total reduction of the Knight shift ΔK. If we take $K_{\rm orb} \sim 0.26\%$ ($H||c$) as obtained in our previous NMR studies [18], after subtracting $K_{\rm dia}$ from ΔK, the reduction of $K_s(T)$ ($\Delta K_s|_{H\|c\ 5\ {\rm T}}$) at the lowest temperature is ∼25% of its normal-state value. This partial decline of $K_s(T)$ suggests an unconventional superconducting pairing with a large amount of residual density of states (DOS) at E_F, e.g., strong Volovik or paramagnetic depairing effect [31,56].

Figures 4(a)–4(h) summarize the results of field-dependent NMR measurements. Two characteristic temperatures can be extracted from these plots. As indicated by the dashed lines in Figs. 4(a)–4(c) and 4(e)–4(g), apparent reductions of Knight shift and linewidth broadenings can be detected below T_c under the external magnetic field $H \leqslant 10$ T. This feature is absent when H is raised up to 12 T. As indicated by the arrows in Figs. 4(a)–4(d), at the measuring magnetic fields, there is another slight decrease of $K(T)$ below a characteristic temperature (denoted as T_p), which is much higher than T_c. Such a behavior is beyond a standard BCS paradigm. FeSe, as a three-dimensional (3D) superconductor, vortex-liquid state only occupies a narrow region in the H-T phase diagram [Fig. 4(i)], and only plays a minor role in NMR experiments. This preempted decrease of the Knight shift is more likely a pseudogap behavior, and similar features have been observed by several experiments in FeSe and its derived systems [11,13,14]. As mentioned above, T_c is the onset temperature of the static vortex-lattice state. The fading away of T_c indicates that $H = 12$ T is very close to the upper critical field (H_{c2}) of the studied enriched sample [28]. In contrast, as rooted in the BCS-BEC crossover regime, the pseudogaplike behavior should be related to the locally preformed Cooper pairs [5,6,11,13,14], which could exist far above T_c. Accordingly, comparing with T_c, T_p is less affected by the external magnetic field, and these two can separate from each other at moderate magnetic fields [13]. As shown in Fig. 4(i), based on previous thermodynamic measurements and the $T_c(H)$, $T_p(H)$ observed in this study, we depict a renewed H-T phase diagram to illustrate the superconducting property of bulk FeSe. In spite of a large uncertainty in the determination of $T_p(H)$, a novel superconducting-fluctuation region between $T_c(H)$ and $T_p(H)$ is clearly revealed. These results are consistent with previous spin-lattice relaxation and thermodynamic characterizations [11–13]. Therefore, the pseudogaplike behavior is also evidenced by our revised NMR spectral measurements at moderate magnetic fields. In Fig. 4(h), taking $H_{c2} = 12$ T, a good scaling relation between the Knight shift $K(H)$ and the specific heat coefficients $\gamma(H)$ in the field range of 5–12 T is obtained. Previously, several experiments suggested a nodal superconducting gap structure [27,28]. To diagnose this proposal, we conduct Knight-shift measurements at sufficiently low fields to check the expected $K(H) \propto \sqrt{H/H_{c2}}$ relation [56]. However, the poor signal to noise ratio of the NMR spectra (<1.5 T) hinders us to make a reliable analysis on this issue. Nevertheless, there is a large amount of residual K_s in the mixed state of superconducting FeSe at high fields.

The superconducting gap structure of bulk FeSe is a hotly debated issue. Since the anisotropic superconducting gap on the Fermi pocket around the Γ point can be well fitted by a p-wave gap function with $\Delta_\Gamma \sim |\Delta_p\cos(\theta)|$, the possibility of p-wave pairing was proposed by only considering previous NMR results [19]. Now, by considering the revised NMR results on the Knight shift in the superconducting state, the chiral p-wave pairing with the $\boldsymbol{d}$ vector pinned along the crystallographic axis or easily reoriented under an external field can be unambiguously ruled out [38]. In fact, within the spin-fluctuation-mediated pairing scenario, IBSCs can hardly possess a p-wave gap symmetry, while $s^{\pm}$- or d-wave pairing is favored [5,23–25,33]. In bulk FeSe, due to the absence of magnetism and the coexistence of $(\pi, 0)$ and (π, π) spin fluctuations, the preempted nematic order parameter $\varphi_{\rm nem} \sim \frac{n_{d_{xz}} - n_{d_{yz}}}{2}$ enables a linear coupling between the comparable s- and d-wave pairing channels [5,23,57], where $n_{d_{xz}}$ and $n_{d_{yz}}$ are the occupation number of the d_{xz} and d_{yz} orbitals. This could yield a complex mixing of s- and d-wave pairing symmetry

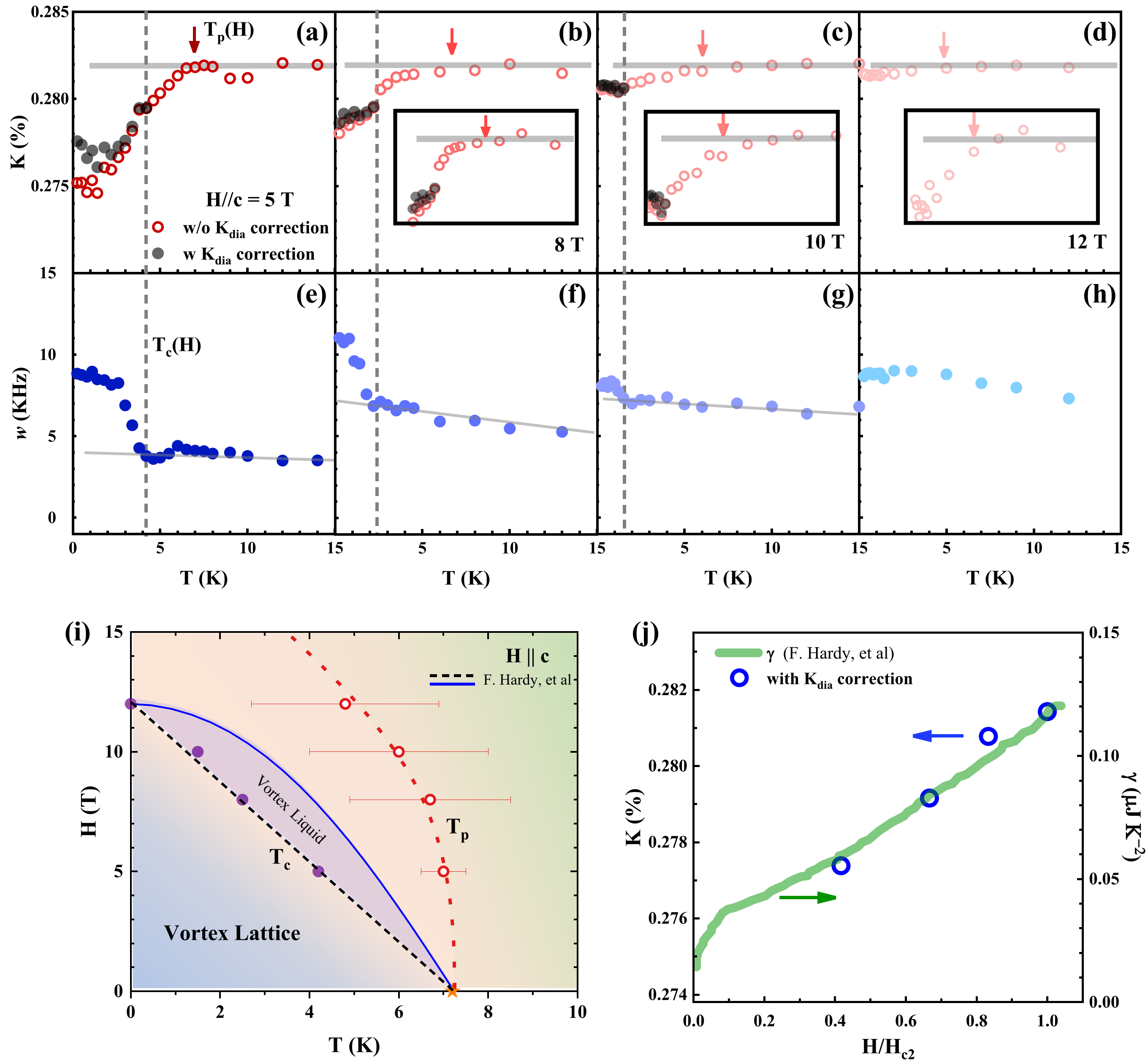

FIG. 4. NMR evidence for exotic superconducting fluctuations above T_c. (a)–(d) $K(T)$ under several external magnetic fields. The insets of (b)–(d) are the zoom-in views of the region around the onset temperature of the slight decline of $K(T)$. (e)–(h) $w(T)$ under several external magnetic fields. (i) A sketch of the superconducting phase diagram of bulk FeSe. The black dashed line and the blue solid line are adapted from Ref. [31]. Note: These data are scaled to match our sample, whose zero field $T_c \sim 7.2$ K and zero temperature $H_{c2} \sim 12$ T. As indicated by the red dotted line, extrapolating the experimental data to the zero-field limit yields $T_c(0) \sim T_p(0)$, which is consistent with the missing pseudogap in the STM/STS and angle-resolved photoemission spectroscopy measurements at zero field [10,19]. The gradient background color indicates a crossover character of the phase diagram. (j) Scaling relation between $K(H)$ and $\gamma(H)$ (reproduced from Ref. [28]) at 0.5 K. Error bars in (i) are defined as the temperature interval of the data around the declining point of $K(T)$.

$\Delta \sim \Delta_s + e^{i\alpha}\Delta_d\cos(2\theta)$ and may lead to a decoupling between nematicity and superconductivity [23]. Such a scenario is supported by our observation: φ_{nem} remains unchanged deep in the superconducting state in stark contrast with the case in $Ba(Fe_{1-x}Co_x)_2As_2$ [58]. Combined with the sign-change character of φ_{nem} at the hole and electron pocket, it was proposed that α could probably deviate from 0 or π through an Ising-type phase transition to maximize the superconducting condensation energy at sufficiently low temperatures in bulk FeSe [25]. Experimental evidences for this transition, e.g., an anomaly in $\gamma(T)$ at ∼1 K, is still under debate [28,59]. Theoretically, the appearance of a nonzero imaginary part in $e^{i\alpha}$ means a TRSB superconducting state ($s + id$-wave pairing), which holds the existence of a spontaneous local field in the region controlled by domain boundaries and defects [6,32,60]. However, within our experimental resolution

($w \sim 8\,\mathrm{KHz} \sim 10\,\mathrm{Oe}$), there is no abrupt broadening associated with the emergence of the TRSB superconducting state, suggesting that if any, an accompanied local field of the putative TRSB state should be rather small [60]. Thus, the existence of a TRSB state is still elusive. Regardless of this issue, note that nodal positions in a mixed $s^{\pm}$- and d-wave gap structure are determined by details of the mixture rather than restricted by symmetry [5]. Controversial conclusions on the gap nodes of bulk FeSe among different spectroscopic or thermodynamic measurements support this idea, since the gap structure of mixed pairing sensitively depends on sample quality [17,28,33]. In our NMR spectral measurements, the incomplete decline of K_s and the good scaling relation between $K(H)$ and $\gamma(H)$ probably reflect a prominent Volovik effect that manifests in an $s^{\pm}$- or d-wave pairing superconducting state [56]. Therefore, the mixing-pairing scenario is a promising candidate [23]. With further NMR investigations, the details of the gap structure, e.g., the weight of $s^{\pm}$- and d-wave pairing, could be determined.

The physics due to the BCS-BEC crossover may also enrich the phase diagram of superconductivity in bulk FeSe, e.g., the existence of locally preformed Cooper pairs [8–14]. Straightforward consequences of such a BEC behavior are the pseudogap in DOS and the anomaly in specific heat above T_c [5,10,61–63]. However, these features are missing in scanning tunneling spectroscopy and thermodynamic measurements [10,31]. One possible reason is the fixing of chemical potential due to the electron-hole compensation in the multiband system bulk FeSe [5,10,61,62]. Nevertheless, in this study, the slight decline of the local spin susceptibility above T_c signals the existence of preformed Cooper pairs at moderate fields. In fact, unlike the enhanced thermal fluctuations in quasi-two-dimensional superconductors, the locally preformed Cooper pairs in the 3D-superconductor bulk FeSe may possess novel pairing fluctuations and open a spin gap to diminish K_s far above T_c, especially in the strong BEC limit [11,13,64]. In addition, in view of the absence of magnetic order, the observed skewed distribution of the NMR spectra in the vortex-lattice state may also be originated from the physics related to the BCS-BEC crossover [49].

IV. CONCLUSION

In conclusion, we successfully obtain intrinsic ^{77}Se NMR spectra in the superconducting state of bulk FeSe with magnetic field along both in-plane and out-of-plane directions. We find obvious reductions of the Knight shift along all directions in the superconducting state, which is consistent with a mixed $s^{\pm}$- and d-wave pairing scenario. Moreover, a slight decline of the Knight shift is already observed far above T_c under a moderate magnetic field, suggesting a pseudogaplike behavior due to exotic superconducting fluctuations. All these renewed NMR results provide valuable hints and constraints for elucidating the exotic superconductivity in bulk FeSe and its derived systems.

ACKNOWLEDGMENTS

This work is supported by the National Key R&D Program of the MOST of China (Grants No. 2017YFA0303000 and No. 2016YFA0300201), the National Natural Science Foundation of China (Grants No. 11888101 and No. 12034004), the Strategic Priority Research Program of Chinese Academy of Sciences (Grant No. XDB25000000), the Anhui Initiative in Quantum Information Technologies (Grant No. AHY160000), and the Collaborative Innovation Program of Hefei Science Center, CAS (Grant No. 2019HSC-CIP007).

[1] M. Sigrist and K. Ueda, Phenomenological theory of unconventional superconductivity, Rev. Mod. Phys. **63**, 239 (1991).

[2] R. M. Fernandes and A. V. Chubukov, Low-energy microscopic models for iron-based superconductors: A review, Rep. Prog. Phys. **80**, 014503 (2016).

[3] G. R. Stewart, Superconductivity in iron compounds, Rev. Mod. Phys. **83**, 1589 (2011).

[4] T. Shibauchi, A. Carrington, and Y. Matsuda, A quantum critical point lying beneath the superconducting dome in iron pnictides, Annu. Rev. Condens. Matter Phys. **5**, 113 (2014).

[5] A. Kreisel, P. J. Hirschfeld, and B. M. Andersen, On the remarkable superconductivity of FeSe and its close cousins, Symmetry **12**, 1402 (2020).

[6] T. Shibauchi, T. Hanaguri, and Y. Matsuda, Exotic superconducting states in FeSe-based materials, J. Phys. Soc. Jpn. **89**, 102002 (2020).

[7] S. Kasahara, T. Watashige, T. Hanaguri, Y. Kohsaka, T. Yamashita, Y. Shimoyama, Y. Mizukami, R. Endo, H. Ikeda, K. Aoyama *et al.*, Field-induced superconducting phase of FeSe in the BCS-BEC crossover, Proc. Natl. Acad. Sci. USA **111**, 16309 (2014).

[8] Q. Chen, J. Stajic, S. Tan, and K. Levin, BCS-BEC crossover: From high temperature superconductors to ultracold superfluids, Phys. Rep. **412**, 1 (2005).

[9] M. Randeria and E. Taylor, Crossover from Bardeen-Cooper-Schrieffer to Bose-Einstein condensation and the unitary Fermi gas, Annu. Rev. Condens. Matter Phys. **5**, 209 (2014).

[10] T. Hanaguri, S. Kasahara, J. Boker, I. Eremin, T. Shibauchi, and Y. Matsuda, Quantum Vortex Core and Missing Pseudogap in the Multiband BCS-BEC Crossover Superconductor FeSe, Phys. Rev. Lett. **122**, 077001 (2019).

[11] S. Kasahara, T. Yamashita, A. Shi, R. Kobayashi, Y. Shimoyama, T. Watashige, K. Ishida, T. Terashima, T. Wolf, F. Hardy *et al.*, Giant superconducting fluctuations in the compensated semimetal FeSe at the BCS–BEC crossover, Nat. Commun. **7**, 12843 (2016).

[12] S. Kasahara, Y. Sato, S. Licciardello, M. Čulo, S. Arsenijević, T. Ottenbros, T. Tominaga, J. Böker, I. Eremin, T. Shibauchi *et al.*, Evidence for an Fulde-Ferrell-Larkin-Ovchinnikov State with Segmented Vortices in the BCS-BEC-Crossover Superconductor FeSe, Phys. Rev. Lett. **124**, 107001 (2020).

[13] A. L. Shi, T. Arai, S. Kitagawa, T. Yamanaka, K. Ishida, A. E. Bohmer, C. Meingast, T. Wolf, M. Hirata, and T. Sasaki, Pseudogap behavior of the nuclear spin-lattice relaxation rate in FeSe probed by ^{77}Se NMR, J. Phys. Soc. Jpn. **87**, 013704 (2018).

[14] B. L. Kang, M. Z. Shi, S. J. Li, H. H. Wang, Q. Zhang, D. Zhao, J. Li, D. W. Song, L. X. Zheng, L. P. Nie *et al.*, Preformed Cooper Pairs in Layered FeSe-Based Superconductors, Phys. Rev. Lett. **125**, 097003 (2020).

[15] A. E. Böhmer and A. Kreisel, The key ingredients of the electronic structure of FeSe, J. Phys.: Condens. Matter **30**, 023001 (2018).

[16] A. Kostin, P. O. Sprau, A. Kreisel, Y. X. Chong, A. E. Böhmer, P. C. Canfield, P. J. Hirschfeld, B. M. Andersen, and J. C. Séamus Davis, Imaging orbital-selective quasiparticles in the Hund's metal state of FeSe, Nat. Mater. **17**, 869 (2018).

[17] P. O. Sprau, A. Kostin, A. Kreisel, A. E. Böhmer, V. Taufour, P. C. Canfield, S. Mukherjee, P. J. Hirschfeld, B. M. Andersen, and J. C. S. Davis, Discovery of orbital-selective cooper pairing in FeSe, Science **357**, 75 (2017).

[18] J. Li, B. Lei, D. Zhao, L. P. Nie, D. W. Song, L. X. Zheng, S. J. Li, B. L. Kang, X. G. Luo, T. Wu, and X. H. Chen, Spin-Orbital-Intertwined Nematic State in FeSe, Phys. Rev. X **10**, 011034 (2020).

[19] D.-F. Liu, C. Li, J. Huang, B. Lei, L. Wang, X. Wu, B. Shen, Q. Gao, Y. Zhang, X. Liu *et al.*, Orbital Origin of Extremely Anisotropic Superconducting Gap in Nematic Phase of FeSe Superconductor, Phys. Rev. X **8**, 031033 (2018).

[20] R. P. Day, G. Levy, M. Michiardi, B. Zwartsenberg, M. Zonno, F. Ji, E. Razzoli, F. Boschini, S. Chi, R. Liang *et al.*, Influence of Spin-Orbit Coupling in Iron-Based Superconductors, Phys. Rev. Lett. **121**, 076401 (2018).

[21] M.-W. Ma, P. Bourges, Y. Sidis, Y. Xu, S.-Y. Li, B.-Y. Hu, J.-R. Li, F. Wang, and Y. Li, Prominent Role of Spin-Orbit Coupling in FeSe Revealed by Inelastic Neutron Scattering, Phys. Rev. X **7**, 021025 (2017).

[22] S. V. Borisenko, D. V. Evtushinsky, Z.-H. Liu, I. Morozov, R. Kappenberger, S. Wurmehl, B. Büchner, A. N. Yaresko, T. K. Kim, M. Hoesch *et al.*, Direct observation of spin-orbit coupling in iron-based superconductors, Nat. Phys. **12**, 311 (2016).

[23] J. Kang, R. M. Fernandes, and A. Chubukov, Superconductivity in FeSe: The Role of Nematic Order, Phys. Rev. Lett. **120**, 267001 (2018).

[24] L. Benfatto, B. Valenzuela, and L. Fanfarillo, Nematic pairing from orbital-selective spin fluctuations in FeSe, Npj Quantum Mater. **3**, 56 (2018).

[25] J. Kang, A. V. Chubukov, and R. M. Fernandes, Time-reversal symmetry-breaking nematic superconductivity in FeSe, Phys. Rev. B **98**, 064508 (2018).

[26] F. Wang and D.-h. Lee, The electron-pairing mechanism of iron-based superconductors, Science **332**, 200 (2011).

[27] P. K. Biswas, A. Kreisel, Q. Wang, D. T. Adroja, A. D. Hillier, J. Zhao, R. Khasanov, J.-C. Orain, A. Amato, and E. Morenzoni, Evidence of nodal gap structure in the basal plane of the FeSe superconductor, Phys. Rev. B **98**, 180501(R) (2018).

[28] F. Hardy, M. He, L. Wang, T. Wolf, P. Schweiss, M. Merz, M. Barth, P. Adelmann, R. Eder, A.-A. Haghighirad, and C. Meingast, Calorimetric evidence of nodal gaps in the nematic superconductor FeSe, Phys. Rev. B **99**, 035157 (2019).

[29] P. Bourgeois-Hope, S. Chi, D. Bonn, R. Liang, W. Hardy, T. Wolf, C. Meingast, N. Doiron-Leyraud, and L. Taillefer, Thermal Conductivity of the Iron-Based Superconductor FeSe: Nodeless Gap with a Strong Two-Band Character, Phys. Rev. Lett. **117**, 097003 (2016).

[30] M. Abdel-Hafiez, J. Ge, A. Vasiliev, D. Chareev, J. Vondel, V. V. Moshchalkov, and A. V. Silhanek, Temperature dependence of lower critical field $H_{c1}(T)$ shows nodeless superconductivity in FeSe, Phys. Rev. B **88**, 174512 (2013).

[31] F. Hardy, L. Doussoulin, T. Klein, M. He, A. Demuer, R. Willa, K. Willa, A.-A. Haghighirad, T. Wolf, M. Merz *et al.*, Vortex-lattice melting and paramagnetic depairing in the nematic superconductor FeSe, Phys. Rev. Research **2**, 033319 (2020).

[32] T. Watashige, Y. Tsutsumi, T. Hanaguri, Y. Kohsaka, S. Kasahara, A. Furusaki, M. Sigrist, C. Meingast, T. Wolf, H. v. Löhneysen *et al.*, Evidence for Time-Reversal Symmetry Breaking of the Superconducting State Near Twin-Boundary Interfaces in FeSe Revealed by Scanning Tunneling Spectroscopy, Phys. Rev. X **5**, 031022 (2015).

[33] T. Hashimoto, Y. Ota, H. Q. Yamamoto, Y. Suzuki, T. Shimojima, S. Watanabe, C. Chen, S. Kasahara, Y. Matsuda, T. Shibauchi *et al.*, Superconducting gap anisotropy sensitive to nematic domains in FeSe, Nat. Commun. **9**, 282 (2018).

[34] S.-H. Baek, D. V. Efremov, J. M. Ok, J. S. Kim, J. van den Brink, and B. Buchner, Orbital-driven nematicity in FeSe, Nat. Mater. **14**, 210 (2015).

[35] A. E. Böhmer, T. Arai, F. Hardy, T. Hattori, T. Iye, T. Wolf, H. v. Lohneysen, K. Ishida, and C. Meingast, Origin of the Tetragonal-to-Orthorhombic Phase Transition in FeSe: A Combined Thermodynamic and NMR Study of Nematicity, Phys. Rev. Lett. **114**, 027001 (2015).

[36] R. X. Cao, Jun Dong, Q. L. Wang, X. S. Ye, J. B. Zhang, Y. F. Xu, D. A. Chareev, A. N. Vasiliev, B. Wu, G. Wu, and X. H. Zeng, Observation of orbital ordering and origin of nematic order in FeSe, New J. Phys. **21**, 103033 (2019).

[37] K. Ishida, M. Manago, K. Kinjo, and Y. Maeno, Reduction of the ^{17}O Knight shift in the superconducting state and the heat-up effect by NMR pulses on Sr_2RuO_4, J. Phys. Soc. Jpn. **89**, 034712 (2020).

[38] A. Pustogow, Y. Luo, A. Chronister, Y.-S. Su, D. A. Sokolov, F. Jerzembeck, A. P. Mackenzie, C. W. Hicks, N. Kikugawa, S. Raghu *et al.*, Constraints on the superconducting order parameter in Sr_2RuO_4 from oxygen-17 nuclear magnetic resonance, Nature (London) **574**, 72 (2019).

[39] See Supplemental Material at http://link.aps.org/supplemental/10.1103/PhysRevB.105.054514 for the experimental settings, simulation details, and the supporting results.

[40] S. Teknowijoyo, K. Cho, M. A. Tanatar, J. Gonzales, A. E. Böhmer, O. Cavani, V. Mishra, P. J. Hirschfeld, S. L. Bud'ko, P. C. Canfield, and R. Prozorov, Enhancement of superconducting transition temperature by pointlike disorder and anisotropic energy gap in FeSe single crystals, Phys. Rev. B **94**, 064521 (2016).

[41] E. H. Brandt, The flux-line lattice in superconductors, Rep. Prog. Phys. **58**, 1465 (1995).

[42] A. Maisuradze, R. Khasanov, A. Shengelaya, and H. Keller, Comparison of different methods for analyzing μSR line shapes in the vortex state of type-II superconductors, J. Phys.: Condens. Matter **21**, 075701 (2009).

[43] R. Khasanov, K. Conder, E. Pomjakushina, A. Amato, C. Baines, Z. Bukowski, J. Karpinski, S. Katrych, H.-H. Klauss, H. Luetkens *et al.*, Evidence of nodeless superconductivity in $FeSe_{0.85}$ from a muon-spin-rotation study of the in-plane magnetic penetration depth, Phys. Rev. B **78**, 220510(R) (2008).

[44] H. Kim, C. Martin, R. T. Gordon, M. A. Tanatar, J. Hu, B. Qian, Z. Q. Mao, R. Hu, C. Petrovic, N. Salovich *et al.*, London penetration depth and superfluid density of single-crystalline $Fe_{1+y}(Te_{1-x}Se_x)$ and $Fe_{1+y}(Te_{1-x}S_x)$, Phys. Rev. B **81**, 180503(R) (2010).

[45] R. X. Cao, J. Dong, Q. L. Wang, Y. J. Yang, C. Zhao, X. H. Zeng, D. A. Chareev, A. N. Vasiliev, B. Wu, and G. Wu, Measurements of the superconducting anisotropy in FeSe with a resonance frequency technique, AIP Adv. **9**, 045220 (2019).

[46] N. J. Curro, B. Simovic, P. C. Hammel, P. G. Pagliuso, J. L. Sarrao, and J. D. Thompson, Anomalous NMR magnetic shifts in $CeCoIn_5$, Phys. Rev. B **64**, R180514 (2001).

[47] V. F. Mitrović, G. Koutroulakis, M. Klanjšek, M. Horvatić, C. Berthier, G. Knebel, G. Lapertot, and J. Flouquet, Comment on "Texture in the Superconducting Order Parameter of $CeCoIn_5$ Revealed by Nuclear Magnetic Resonance, Phys. Rev. Lett. **101**, 039701 (2008).

[48] S.-H. Baek, D. V. Efremov, J. M. Ok, J. S. Kim, J. van den Brink, and B. Büchner, Nematicity and in-plane anisotropy of superconductivity in β-FeSe detected by ^{77}Se nuclear magnetic resonance, Phys. Rev. B **93**, 180502 (2016).

[49] I. Vinograd, S. P. Edwards, Z. Wang, T. Kissikov, J. K. Byland, J. R. Badger, V. Taufour, and N. J. Curro, Inhomogeneous Knight shift in vortex cores of superconducting FeSe, Phys. Rev. B **104**, 014502 (2021).

[50] V. F. Mitrović, E. E. Sigmund, M. Eschrig, H. N. Bachman, W. P. Halperin, A. P. Reyes, P. Kuhns, and W. G. Moulton, Spatially resolved electronic structure inside and outside the vortex cores of a high-temperature superconductor, Nature (London) **413**, 501 (2001).

[51] A. V. Putilov, C. D. Giorgio, V. L. Vadimov, D. J. Trainer, E. M. Lechner, J. L. Curtis, M. Abdel-Hafiez, O. S. Volvoka, A. N. Vasiliev, D. A. Chareev *et al.*, Vortex core properties and vortex-lattice transformation in FeSe, Phys. Rev. B **99**, 144514 (2019).

[52] N. Schopohl and A. Baratoff, Magnetic properties of anisotropic extreme type-II superconductors, Physica C **153**, 689 (1988).

[53] C. G. Wang, Z. Li, J. Yang, L. Y. Xing, G. Y. Dai, X. C. Wang, C. Q. Jin, R. Zhou, and G.-q. Zheng, Electron Mass Enhancement near a Nematic Quantum Critical Point in $NaFe_{1-x}Co_xAs$, Phys. Rev. Lett. **121**, 167004 (2018).

[54] S. Oh, A. M. Mounce, S. Mukhopadhyay, W. P. Halperin, A. B. Vorontsov, S. L. Bud'ko, P. C. Canfield, Y. Furukawa, A. P. Reyes, and P. L. Kuhns, ^{75}As NMR of $Ba(Fe_{0.93}Co_{0.07})_2As_2$ in high magnetic field, Phys. Rev. B **83**, 214501 (2011).

[55] K. Matano, M. Kriener, K. Segawa, Y. Ando, and G.-q. Zheng, Spin-rotation symmetry breaking in the superconducting state of $Cu_xBi_2Se_3$, Nat. Phys. **12**, 852 (2016).

[56] Y. Bang, Volovik effect on NMR measurements of unconventional superconductors, Phys. Rev. B **85**, 104524 (2012).

[57] R. M. Fernandes and A. J. Millis, Nematicity as a Probe of Superconducting Pairing in Iron-Based Superconductors, Phys. Rev. Lett. **111**, 127001 (2013).

[58] S. Nandi, M. G. Kim, A. Kreyssig, R. M. Fernandes, D. K. Pratt, A. Thaler, N. Ni, S. L. Bud'ko, P. C. Canfield, J. Schmalian *et al.*, Anomalous Suppression of the Orthorhombic Lattice Distortion in Superconducting $Ba(Fe_{1-x}Co_x)_2As_2$ Single Crystals, Phys. Rev. Lett. **104**, 057006 (2010).

[59] G. Y. Chen, X. Zhu, H. Yang, and H. H. Wen, Highly anisotropic superconducting gaps and possible evidence of antiferromagnetic order in FeSe single crystals, Phys. Rev. B **96**, 064524 (2017).

[60] S.-Z. Lin, S. Maiti, and A. Chubukov, Distinguishing between $s+id$ and $s+is$ pairing symmetries in multiband superconductors through spontaneous magnetization pattern induced by a defect, Phys. Rev. B **94**, 064519 (2016).

[61] A. V. Chubukov, I. Eremin, and D. V. Efremov, Superconductivity versus bound-state formation in a two-band superconductor with small Fermi energy: Applications to Fe pnictides/chalcogenides and doped $SrTiO_3$, Phys. Rev. B **93**, 174516 (2016).

[62] S. Rinott, K. B. Chashka, A. Ribak, E. D. L. Rienks, A. Taleb-Ibrahimi, P. Le Fevre, F. Bertran, M. Randeria, and A. Kanigel, Tuning across the BCS-BEC crossover in the multiband superconductor $Fe_{1+y}Se_xTe_{1-x}$: An angle-resolved photoemission study, Sci. Adv. **3**, 1602372 (2017).

[63] P. van Wyk, H. Tajima, R. Hanai, and Y. Ohashi, Specific heat and effects of pairing fluctuations in the BCS-BEC-crossover regime of an ultracold Fermi gas, Phys. Rev. A **93**, 013621 (2016).

[64] H. Tajima, T. Kashimura, R. Hanai, R. Watanabe, and Y. Ohashi, Uniform spin susceptibility and spin-gap phenomenon in the BCS-BEC-crossover regime of an ultracold Fermi gas, Phys. Rev. A **89**, 033617 (2014).